ISBN: 978-3-95450-247-9 ISSN: 2673-5490 doi: 10.18429/JACoW-IPAC2024-TUPS38

ENERGY DEPOSITION IN THE NEW SPS's SCRAPERS

S. Niang*, L. S. Esposito, CERN, Geneva, Switzerland

Abstract

The successful injection of proton beams into the Large Hadron Collider (LHC) depends on an efficient scraping mechanisms in the Super Proton Synchrotron (SPS). The beams accelerated in the SPS contain a significant non-Gaussian tail population. If not removed, this transverse tail population can cause high losses in the transfer lines and in the LHC injection elements. Subsequently, the Beam Loss Monitor (BLM) system may trigger a beam dump reducing the machine availability. As beam intensities increase to meet the parameters set by the LHC Injector Upgrade (LIU), the efficiency of the scraping operation becomes increasingly crucial.

To fully cope with higher beam intensities in the framework of the High-Luminosity LHC (HL-LHC) project, an upgrade of the scraper system, consisting of two movable graphite blade, is been developed and scheduled for installation in January 2025. This article presents the results of two comprehensive simulation studies aiming to assess energy deposition in the scrapers. These simulations employ the `FLUKA` code coupled with `SixTrack` for the first one and with `Xsuite` for the second one.

INTRODUCTION

During the first run of the Large Hadron Collider (LHC) [1–3], it was observed that injecting multi-bunch LHC beams into the collider was not possible without eliminating transverse tails in the Super Proton Synchrotron (SPS) through transverse scraping. This necessity arises from the losses caused by beam tails that, during injection into the LHC, would surpass the dump thresholds set by the LHC Beam Loss Monitor (BLM) system and potentially damage the machine. Scraping all high-intensity LHC beams is imperative, and this becomes even more crucial as beam intensities are pushed towards the LHC Injector Upgrade (LIU) parameter regime [4, 5] to meet the performance goals of the High-Luminosity LHC (HL-LHC) [6].

Currently, two scrapers denoted as `BSHV.11771` and `BSHV.11772` and separated by less than a meter are situated in the SPS accelerator ring. The complete characterisation of the current beam scraping system is thoroughly documented in [7, 8]. A new (forth) generation scraper is currently under design [9] to cope with increased number of cycles and higher intensity beams. Following the functional specification [10], the scraper should be capable of sustaining a full beam at the flat top, *i.e.* 9.6×10^{13} protons with a momentum of 450 GeV/c for a few cycles. The entire scraping movement shall be executed within 100 ms. Given the small distance between the scrapers, our attention will be directed exclusively towards the first one, identified as `BSHV.11771`.

This proceeding presents the results of the energy deposition studies in the blade, which serve as input for a broader feasibility analysis of the thermo-mechanical aspects of the blade. This results are obtained with `FLUKA` [11–13] coupled with two multi-turn tracking tools. The first simulation integrates `FLUKA` with `SixTrack` [14–16], while the second one with `Xsuite` [17, 18].

In both simulation frameworks, `FLUKA` models the interactions of particles with the scraper blade, while `SixTrack` or `Xsuite` track the particles in the rest of the SPS ring outside of the scraper area.

`SixTrack` simulates the trajectory of beam particles throughout the accelerator lattice. In contrast, `Xsuite` is a modern Python toolkit developed at CERN to simulate particle behaviour in an accelerator, aiming at integrating existing tools for different applications into a single framework.

`FLUKA` identifies and returns the surviving protons to `SixTrack` or `Xsuite` for successive, turn-by-turn tracking. Although the codes run independently when coupled, they are configured to exchange particle information dynamically during runtime.

PARAMETERS OF THE SIMULATION

The scraper should be usable along the full cycle, with a momentum from 26 GeV/c up to 450 GeV/c. In this study, focusing on the worst case, we examine an SPS beam operating at its maximum energy, denoting a proton beam with a momentum of 450 GeV/c. The Twiss parameters at the scraper location are outlined in Table 1, and the (1σ) normalised emittance value (horizontal and vertical) is set at $\epsilon_n = 2.0 \times 10^{-6}$ rad with a momentum variation of $\delta p/p\ (1\sigma) = 2.0 \times 10^{-4}$. These parameters are used to generate the initial particle distribution. The beam size is $\sigma_x = 518$ µm and $\sigma_y = 497$ µm.

Table 1: Twiss Parameters at the Entrance of the Scraper `BSHV.11771`

Horizontal		Vertical	
α_x	−1.2385	α_y	1.2437
β_x	58.867 m	β_y	59.323 m
D_x	−0.753 35	D_y	0
$D_{x'}$	−0.017 795	$D_{y'}$	0

As depicted in Fig. 1, the scraper consists of two blades, each measuring 5 cm × 5 cm × 1 cm. These blades are made of graphite, characterised by a density of 1.83 g cm^{-3}. During normal operation, the blades shall be designed to handle 10% of a proton beam with a total of 9.6×10^{13} protons, as specified in Ref. [10]. However, as mentioned in the intro-

* samuel.niang@cern.ch

ISBN: 978-3-95450-247-9 ISSN: 2673-5490 doi: 10.18429/JACoW-IPAC2024-TUPS38

duction, they should be able to tolerate full beam scraping for a few cycles,, which might happens in case of multiple system failure or erroneous settings.

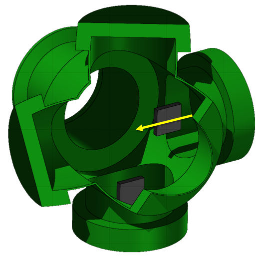

Figure 1: 3D visualisation of the FLUKA model using FLAIR [19].

MOVEMENT OF THE BLADE

The movement of each blade involves travelling both forward and backward, covering a distance of approximately 10 cm, as illustrated by the curves in Fig. 2. The movement is completed within 100 ms.

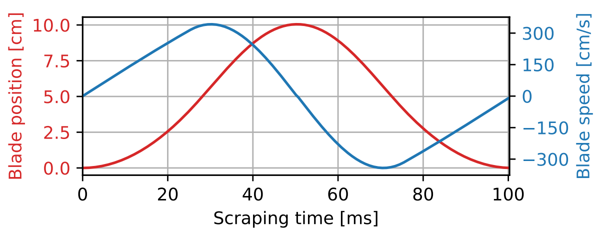

Figure 2: Blade position (red) and blade speed (blue) as a function of the scraping time.

Basically, the operational parameter for modifying the percentage of scraped protons is the initial position of the blade, as shown detailed in Fig. 3. This figure illustrates the percentage of remaining circulating protons as function of x_0, representing the initial distance of the blades from the beam centre (assumed at the centre of the tank).

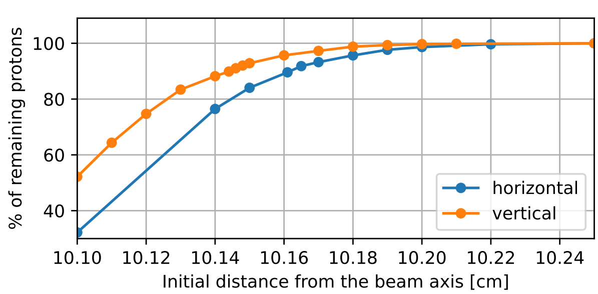

Figure 3: Percentage of remaining circulating protons as a function of the initial position of the blades for the simulation coupling SixTrack and FLUKA.

Achieving a scraping efficiency of 10% requires positioning the blade at approximately 2σ from the beam centre, which corresponds to $\sim$ 0.1 cm, aligning with the values reported in Table 2.

Table 2: Final Position of the Blade with Respect to the Beam Axis in the Different Simulations and Corresponding Number of Scraped Protons

Code	Blade	Δ x [cm]	% scraped
SixTrack	Horizontal	0.112	10.19 ± 0.24
SixTrack	Horizontal	−0.210	99.97 ± 0.01
SixTrack	Vertical	0.095	9.97 ± 0.45
SixTrack	Vertical	−0.193	99.94 ± 0.03
Xsuite	Horizontal	0.097	10.06 ± 0.31
Xsuite	Horizontal	−0.210	99.81 ± 0.04

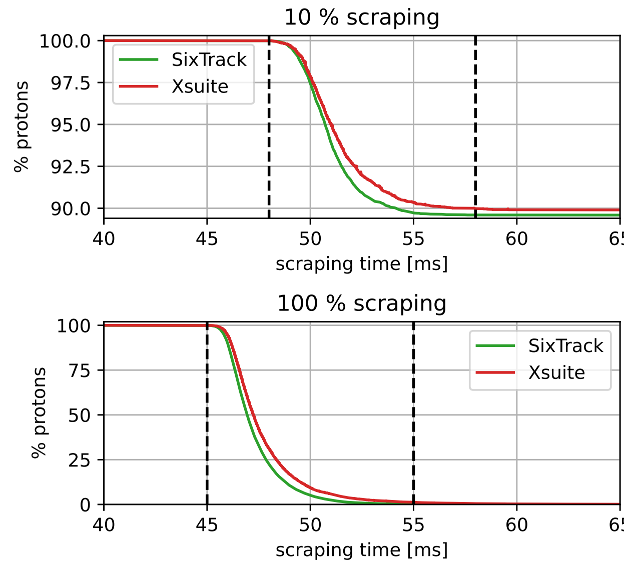

Figure 4: Remaining circulating protons as a function of the scraping time. The dashed lines indicate a time window of 10 ms.

Figure 4 provides a time-wise illustration of the scraping process. Firstly, regardless of the considered scenario, protons interact with the blade for approximately 10 ms. Secondly, it is observed that SixTrack predicts a faster scraping process compared to Xsuite. This is explained by the fact that the Xsuite simulation shows fewer losses in the rest of the accelerator, consistent with its higher estimated energy deposition in the blade, and will be further investigated.

ENERGY DEPOSITION

Figure 5 presents the average energy deposition across the thickness of the blade, while Fig. 6 shows the peak energy deposition profile in the blade along the x-axis.

It is noteworthy to observe that the profile of the maximum energy deposition density per scraped proton along the blade remains consistent regardless of the simulation code employed. This consistency is anticipated, as both simulation codes are designed to accurately model the accelerator and the transport of the beam core.

The specific numerical results obtained from our simulations are summarised in Table 3. In the SixTrack simulation, we observe a total energy deposition in the blade of

ISBN: 978-3-95450-247-9 ISSN: 2673-5490 doi: 10.18429/JACoW-IPAC2024-TUPS38

approximately 165 MeV per scraped proton, while the total energy deposition in the tank is around 100 MeV per proton. In total, ≈ 0.06% of the beam energy is absorbed by the scraper and its tank.

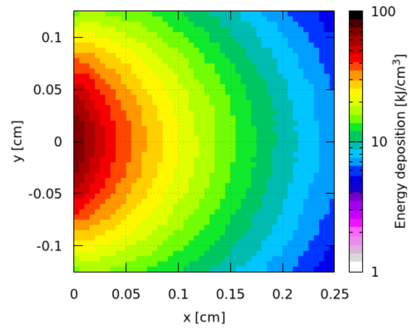

Figure 5: Energy deposition in the horizontal blade when 100% of the protons have been scraped. Normalised to 9.6×10^{13} protons.

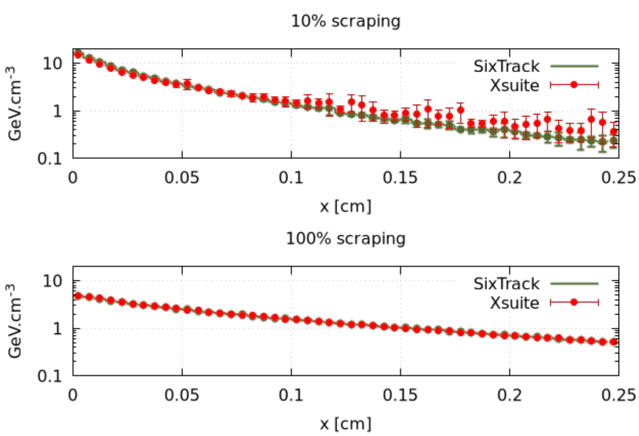

Figure 6: Peak energy deposition profile per scraped proton in the horizontal blade.

Similar results are obtained with coupling with `Xsuite` simulation toolkit. The total energy deposited in the scraper is estimated to be approximately +20% higher compared to the `SixTrack` simulation. As anticipated, this difference is attributed to the fewer losses in the rest of the accelerator, and will be further investigated.

Additionally, from the data presented in both tables and depicted in Fig. 6, it is evident that the maximum energy deposition per scraped proton is approximately 16 GeV cm^{-3} for the 10% scraping scenario, and 5 GeV cm^{-3} for the full scraping scenario. These values align closely with those reported in previous studies [8]. This difference in energy density peak is attributed to the velocity of the blade, which approaches zero during the 10% scraping scenario when the blade first intersects with the beam.

Considering a beam with 9.6×10^{13} circulating protons, we obtain energy depositions around 25 kJ cm^{-3} (10% scraping) and 75 kJ cm^{-3} (10% scraping), significantly exceeding the sublimation heat, which was determined to be 13.2 kJ. This value corresponds to the energy required to heat graphite to its sublimation temperature (3600 °C) from room temperature (25 °C), assuming an adiabatic temperature increase and using the specific heat capacity values cited in Ref. [20].

Despite recognising that the energy deposition process, lasting approximately 10 ms, cannot be strictly considered adiabatic, those values are compatible with local material sublimation,as was the case with the study of the present scraper model [8]. Dedicated thermo-mechanical analysis are still on going to validated the design of the new scraper.

Table 3: Energy deposition and maximal energy density per scraped proton and for a 9.6×10^{13} proton beam. The values are consistent to the ones presented in Table IX of Ref. [8]
.

Case	En. deposition		Max. density	
	scr. pr. [MeV]	beam [kJ]	scr. pr. [GeV cm^{-3}]	beam [kJ cm^{-3}]
`SixTrack`				
H 10%	166	0.25	16.2	24.9
H 100%	168	2.58	4.76	73.1
V 10%	162	0.25	15.3	23.5
V 100%	168	2.55	4.75	73.1
`Xsuite`				
H 10%	194	0.30	15.2	23.4
H 100%	197	3.03	4.89	75.2

CONCLUSION

In this paper, we have reported the results of the energy deposition in the blades of the newly designed SPS scraper, utilising [7] the `FLUKA` code coupled with `SixTrack`. Our findings are consistent with previous studies, showcasing the robustness of our methodology. Furthermore, we have compared those results with a novel coupling framework employing `FLUKA` with `Xsuite`, yielding consistent results across both simulation codes.

The larger total energy deposition calculated by the coupling with `Xsuite` is likely caused by reduced losses along the accelerator ring compared to `SixTrack`. Consequently, more protons, scattered the first time by the scraper, are being redirected back to the scraper, resulting in a higher energy deposition in the blades. This will be object of further investigation.

Throughout the scraping process, spanning approximately 10 ms, each scraped proton contributes to an energy deposition of approximately 195 MeV. Given the specified beam parameters, this is compatible with local sublimation of graphite, as reported in previous study of the present scraper model. The results of our simulations serve as valuable inputs for subsequent thermo-mechanical investigations and validation of the scraper design.

ACKNOWLEDGEMENTS

We would like to thank R. De Maria, G. Hugo and F. F. Van der Veken for their help and support with `Xsuite` and the coupling with `FLUKA`.

ISBN: 978-3-95450-247-9 ISSN: 2673-5490 doi: 10.18429/JACoW-IPAC2024-TUPS38

REFERENCES

[1] M. Facchini, C. Fischer, J. J. Gras, S. Hutchins, and R. Jung, "Scraping for LHC and collimation tests in the CERN SPS," 2005. https://cds.cern.ch/record/895153

[2] L. Drøsdal *et al.*, "Beam stability and tail population at sps scrapers," 2012. https://accelconf.web.cern.ch/HB2012/papers/mop247.pdf

[3] L. Drøsdal *et al.*, "SPS Scraping and LHC Transverse Tails," in *4th International Particle Accelerator Conference*, 2013, MOPWO032.

[4] *LHC Injector Upgrade Project*. https://espace.cern.ch/liu-project/default.aspx

[5] *Liu proton beam parameters*. https://edms.cern.ch/document/1296306/2

[6] *High Luminosity LHC Project*. https://hilumilhc.web.cern.ch

[7] A. Mereghetti, "Performance Evaluation of the SPS Scraping System in View of the High Luminosity LHC," Presented 09 Jun 2015, Manchester U., 2015. https://cds.cern.ch/record/2045506

[8] A. Mereghetti, F. Cerutti, and R. B. Appleby, "Characterization of the beam scraping system of the cern super proton synchrotron," *Phys. Rev. Accel. Beams*, vol. 24, p. 043 002, 4 2021. doi:10.1103/PhysRevAccelBeams.24.043002

[9] E. Grenier-Boley and I. Z. Johansen, "Functional analysis for operational sps scraper," CERN, Tech. Rep., 2023. https://edms.cern.ch/document/2757827/0.1

[10] E. Veyrunes and K. Li, "Functional specification for operational sps scraper," CERN, Tech. Rep., 2023. https://edms.cern.ch/document/2407464/1.0

[11] Fluka. https://fluka.cern/

[12] C. Ahdida *et al.*, "New capabilities of the FLUKA multipurpose code," *Front. Phys.*, vol. 9, 2022. doi:10.3389/fphy.2021.788253

[13] G. Battistoni *et al.*, "Overview of the FLUKA code," *Annals of Nuclear Energy*, vol. 82, pp. 10–18, 2015, Joint International Conference on Supercomputing in Nuclear Applications and Monte Carlo 2013, SNA + MC 2013. Pluri- and Trans-disciplinarity, Towards New Modeling and Numerical Simulation Paradigms. doi:10.1016/j.anucene.2014.11.007

[14] R. D. Maria *et al.*, "SixTrack Version 5: Status and New Developments," in *Proc. IPAC'19*, Melbourne, Australia, May 2019, pp. 3200–3203. doi:10.18429/JACoW-IPAC2019-WEPTS043

[15] A. Mereghetti *et al.*, "SixTrack-FLUKA Active Coupling for the Upgrade of the SPS Scrapers," in *Proc. IPAC'13*, Shanghai, China, May 2013, 2013, pp. 2657–2659. https://jacow.org/IPAC2013/papers/WEPEA064.pdf

[16] "ICFA Mini-Workshop on Tracking for Collimation in Particle Accelerators," 10.23732/CYRCP-2018-002, 2018. https://cds.cern.ch/record/2646800

[17] *Xsuite*. https://xsuite.web.cern.ch

[18] G. Iadarola *et al.*, "Xsuite: An Integrated Beam Physics Simulation Framework," in *Proc. HB'23*, Geneva, Switzerland, Oct. 2024, TUA2I1. doi:10.18429/JACoW-HB2023-TUA2I1

[19] V. Vlachoudis, "Flair: A powerful but user friendly graphical interface for FLUKA," in *Proc. Int. Conf. on Mathematics, Computational Methods & Reactor Physics (M&C 2009)*, 2009. https://cds.cern.ch/record/2749540

[20] "Specific heat capacity," CERN, Tech. Rep. https://edms.cern.ch/document/2933785/1